Origin of arc shape of LEED streaks on Li adsorbed on Cu(001) surface at lower coverage

2006 J. Phys.: Condens. Matter 18 5057

(http://iopscience.iop.org/0953-8984/18/22/006)

INSTITUTE OF PHYSICS PUBLISHING JOURNAL OF PHYSICS: CONDENSED MATTER

J. Phys.: Condens. Matter **18** (2006) 5057–5067 doi:10.1088/0953-8984/18/22/006

Origin of arc shape of LEED streaks on Li adsorbed on Cu(001) surface at lower coverage

Hisashi Mitani[1], **Tohru Hayashi**[2], **Seigi Mizuno**[3] **and Hiroshi Tochihara**[3]

[1] Department of Physics, Fukuoka University of Education, Munakata, Fukuoka 811-4192, Japan
[2] Department of Chemistry, Okayama University, Okayama 816-8580, Japan
[3] Department of Molecules and Material Science, Kyushu University, Kasuga, Fukuoka 700-0082, Japan

Received 30 September 2005, in final form 27 March 2006
Published 16 May 2006
Online at stacks.iop.org/JPhysCM/18/5057

Abstract

We considered the origin of the arc-shaped streaks connecting usual diffraction spots observed in an LEED pattern, for a Li system adsorbed on a Cu(001) surface at low coverage, $\Theta < 1/2$. We noted a condition that the natural distance between adsorbed atoms, b_{nat}, of less than $\sqrt{2}a$—in particular, $b_{\mathrm{nat}} \cong 1.39a$—is consistent with the formation of the arced streaks. Given this condition, adsorbed atoms fill the surface and form a c($5\sqrt{2} \times \sqrt{2}$)R45° structure, which is one of the 'ladder structures', at $\Theta = 3/5$. Even for $\Theta < 1/2$, the atoms form the ladder structure locally. We could observe atomic pairs with second-neighbour distance having a c(2×2) structure unit in the ladder structure (where the distance is basically $d = 2a$), that were shrunk and tilted. These shrunk and tilted pairs produce straight streaks extending from the M($\pm 1/2, \pm 1/2$) points, with a tilted angle in the vicinity of M points. Considering the other arrangements of the second-neighbour pairs, which have a different inclination, a variety of straight streaks exists. The envelope function of these straight streaks is nothing but the arc shape observed in the experiment.

1. Introduction

Ordered structures with super-cells on simple metal monolayer atoms have been observed to adsorb on transition metal surfaces; in particular, Li on Ni(001) [1], Mg on Cu(001) [2], and Li on Cu(001) have been observed experimentally by low-energy electron diffractions (LEED). First, several spots were observed in diffraction spaces; then super-cell structures were proposed. These systems show essentially similar structures.

The systems have been interpreted theoretically as physisorption systems such as the Frenkel–Kontorova model with mutual interactions among adsorbed atoms and a substrate potential [2, 3].

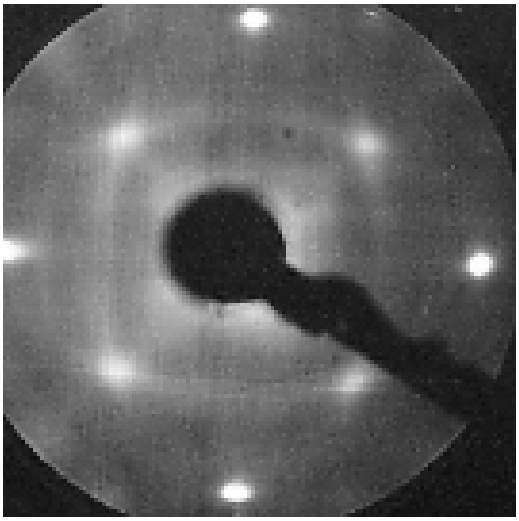

Figure 1. A normal incidence LEED pattern of a Cu(001)–Li surface from [8]. The coverage Θ is 0.23 and the electron beam energy is 53 eV.

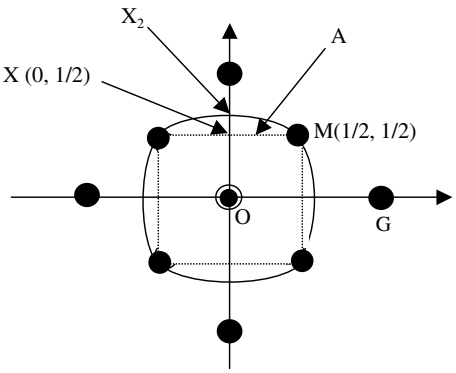

Figure 2. Schematic picture of observed arced streaks from [4]. Solid curves represent arced streaks. Dashed lines with a square type originate from lattice plane sets with the spacing of $d_y = 2a$ as shown in figure 3(a).

On the other hand, a ring streak has been observed in K on Cu(001) surface at lower coverage, which corresponds to the early stage of evaporation [4]. Line streaks have been observed in alkali metals adsorbed on the transition metal fcc(110) 2×1 surface structure, including K on the Cu(110) surface [5]. Besides, the Si(001) c(4×2) surface structure [6], and Bi on Cu(001) [7] showed also line streaks.

We guess the origin of these streaks as follows. The ring streak can be considered to correspond a stable distance between K atoms. The line streaks of K on the Cu(110) and also the Si(001) c(4×2) surface originate from a structural fluctuation or atomic arrays in a one-dimensional direction. We will mention the origin of the streaks of Bi on Cu later.

Recently, arc-shaped streaks connecting the diffraction spots have been observed by LEED in Li on Cu(001) at a low coverage, $\Theta < 1/2$ [8] (see figures 1 and 2). As we mentioned first, Li on Ni(001), Mg on Cu(001), and Li on Cu(001) are essentially similar systems; however, the

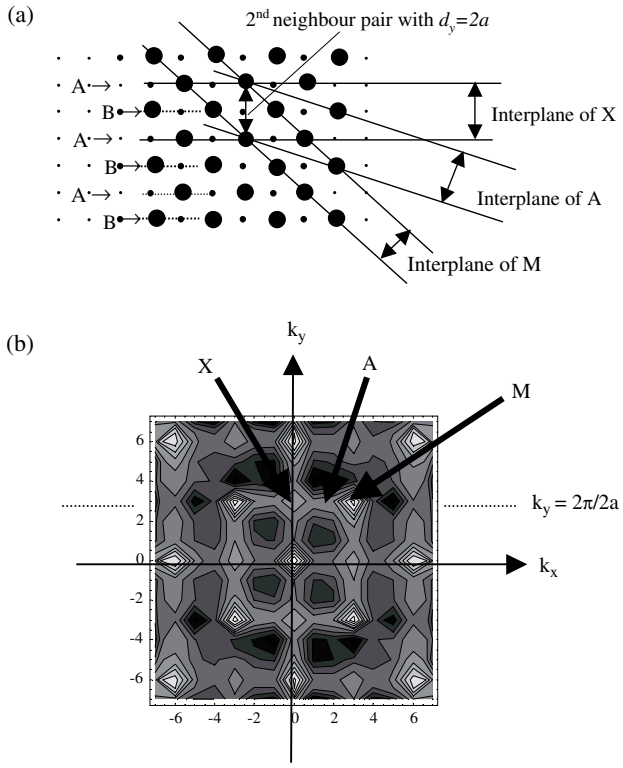

Figure 3. (a) A finite cluster of c(2 × 2) structures of adatoms. Lattice 'planes' (parallel lines) correspond to special points or lines in k-space in (b). The small dots represent adsorbed sites on the Cu (001) surface; on the other hand, big closed circles represent adatoms. 'A' and 'B' represent two types of sublattices of lattice sets. (b) The intensity value of the structure factor from [4]. The calculation is based on equation (1) from the atomic arrangement in (a). Notice that the straight pattern is identified with an array of several points because the system is a finite lattice.

arced streak cannot be seen other than in Li on Cu. Furthermore, there are few systems with the arced streak in any surface systems.

In this paper, we will analyse especially the arc shape in the diffraction space of Li on a Cu(001) surface.

The essential origin of the streaks has already been explained in [8], at least in the case when streaks are straight lines of a square shape, which form square-type streaks. An origin of the rhombic type of streaks of Bi on Cu can be essentially explained by a similar mechanism introduced in [8]. We consider that the arc shape is a deformation of the square-type shape (see figure 2). In this section, we briefly review the origin of the square-type streaks according to [8]; in the following sections, we consider the mechanism by which streaks are deformed from lines to arcs.

We have shown in [8] that a finite c(2×2) cluster (figure 3(a)) produces an intense structure factor with square-type (i.e. four lines) streaks in k-space (figure 3(b)). Hereafter, the structure factor is calculated as

$$S(\vec{k}) = \sum_j \mathrm{e}^{\mathrm{i}\vec{k}\cdot\vec{r}_j}, \tag{1}$$

where r_j is an atomic position, and the intensity is given by $I(\vec{k}) = |S(\vec{k})|^2$.

For example, one streak that locates at $k_y = 2\pi/2a$ in figure 3(b) originates from a pair with two atoms at a separation, $d = 2a$, that is a second-neighbour distance of the c(2 × 2) structure unit (see figure 3(a)).

On a diffraction spot M($\pm 1/2, \pm 1/2$), which originates from reflections of interplane distance with a spacing $d = \sqrt{2}a$, reflected electron waves accumulate and make strong spots in any conditions (see figure 3(b)). Meanwhile, a lattice spacing with $d_y = 2a$ gives a structure factor at line M–X–M, with two opposite phase shifts, $\phi = 0$ and $\phi = \pi$. These shifts originate from two types of planes, sublattices 'A' and 'B' (see figure 3(a)). (Throughout the present paper, we call a one-dimensional array of atoms on a surface, on which electron beams reflect, a 'plane', according to the conventional phrase of a 'Bragg diffraction plane', although it is actually a one-dimensional line.)

For example, the structure factor around point X is

$$\begin{aligned} S(0,0,k_y) &= (N_0^{\mathrm{A}} \mathrm{e}^{\mathrm{i}k_y 0} + N_1^{\mathrm{A}} \mathrm{e}^{\mathrm{i}k_y 2a} + \cdots) + (N_0^{\mathrm{B}} \mathrm{e}^{\mathrm{i}k_y a} + N_1^{\mathrm{B}} \mathrm{e}^{\mathrm{i}k_y 3a} + \cdots) \\ &= (N^{\mathrm{A}} \mathrm{e}^{\mathrm{i}0} + N^{\mathrm{B}} \mathrm{e}^{\mathrm{i}\pi}) \times \delta_{k_y, 2\pi/2a} = (N^{\mathrm{A}} - N^{\mathrm{B}}) \times \delta_{k_y, 2\pi/2a}. \end{aligned} \tag{2}$$

Here we define $N^{\mathrm{A}} = N_0^{\mathrm{A}} + N_1^{\mathrm{A}} + \cdots$, and $N^{\mathrm{B}} = N_0^{\mathrm{B}} + N_1^{\mathrm{B}} + \cdots$. Therefore, the complete c(2 × 2) structure, where $N_0^{\mathrm{A}} = N_1^{\mathrm{A}} = \cdots = N_0^{\mathrm{B}} = N_1^{\mathrm{B}} = \cdots$, does not show any pattern. In other words, reflected waves cancel each other. By contrast, adsorbed atoms with incomplete occupancy show the pattern at $k_y = 2\pi/2a$ (see figure 3(b)). The fluctuation of numbers of type-A and type-B atoms can be calculated using statistics. The fluctuation depends on the coverage. Since the intensity of the streak is proportional to the fluctuation, the coverage dependence of the intensity can be obtained, as described in [8].

2. Origin of the deformation of the streaks

Hereafter, we consider the reason for the deformation of the streaks. We can point out the deformation in the diffraction space as follows. The distance of an X-point from the original O-point is enlarged in the k_y-direction from that in the square streaks. This results in a shrinking of the interplane distance along the y-direction in real space. On the other hand, the edges of the streaks are still located on M-points in the diffraction space (see figure 2). Specifically, a streak extends from an M-point along a straight line with a tilted angle in the vicinity of M points. We can see the above phenomena can be explained by the shift of adsorbed atoms in a c(2 × 2) square unit; one atom moves from a vertex of the square to a point on a side of the square (see figure 4).

Namely, the separation of the pair of atoms, which originally has a second-neighbour distance of c(2 × 2) units, becomes $d_y < 2a$, where we define $d_y = (1/\alpha_1) \times 2a$ ($\alpha_1 \cong 7/5 = 1.40$) in the y-direction. Meanwhile, the separation in the M-direction does not change ($d = \sqrt{2}a$). The composition of the separation changes as the angle of the wave plane is gradually inclined. In a diffraction space, the diffraction point is not moved in the M-direction, while it is enlarged in the X-direction (y-direction), from the X-point at $k_y = 2\pi/2a$ to the X_1-point at $k_y = \alpha_1 \times 2\pi/2a$ (see figure 5). This fact brings about the deformation of the streak. (The fact that the streak is not yet an arc, but a straight line as in figure 5 at this stage, will be discussed later.)

3. Stability and coherency of the deformation of the atomic pairs

The above explanation of the streaks is merely based on an assumption about the tilted and shrunk arrangement of one pair with two atoms as in figure 4. We must clarify the stability

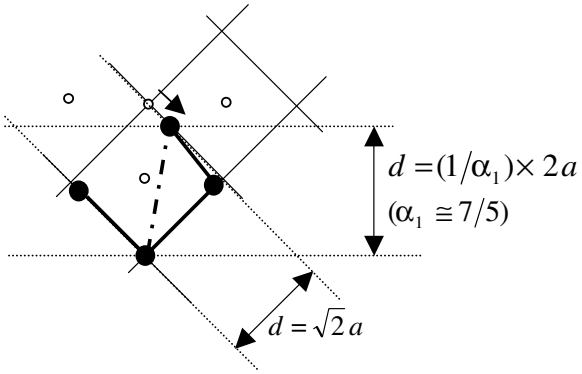

Figure 4. Shrunk and tilted atomic pairs with a second-neighbour relation ($d_y \leqslant 2a$) on a c(2 × 2) structure unit (see a dashed and dotted line).

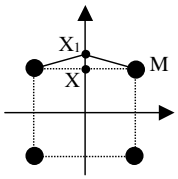

Figure 5. The diffraction pattern obtained from the atomic pairs in figure 4 (note: there must be eight lines for fourfold symmetry; however, we have simplified them).

of this arrangement and explain the intensity and sharpness in the diffraction space in the experiment.

First, we must explain the reasons why such deformations of the second neighbour pairs of the c(2 × 2) unit occur stably in so many places. Second, we must explain the coherency of the diffraction by these pairs.

The reason for the stability of the arrangement is in formation of 'ladder' structures, especially the c($5\sqrt{2} \times \sqrt{2}$)R45° structure. We can discuss the problem as follows. Since a second neighbour pair of a c(2 × 2) unit must be shrunk to explain the deformation of the streaks, the natural distance b_{nat} between the adsorbed atoms is slightly shorter than the nearest-neighbour distance of the c(2 × 2) structure, $d = \sqrt{2}a$ (see figure 4).

Thus, it might be that $a < b_{\mathrm{nat}} < \sqrt{2}a$. This means that a 'bond' with '$d = a$' also exists (notice that the length '$d = a$' indicates a unit length between adsorbed lattice points on the Cu(001) surface; the actual bond length must be slightly larger than '$d = a$'). Then two types of bond lengths, '$d = a$' and '$d = \sqrt{2}a$', exist. A structure including these bonds must be related to the c($n\sqrt{2} \times \sqrt{2}$)R45° structure, which we have named a 'ladder structure', with the coverage, $\Theta = 2/3, 3/5, 4/7, 5/9$, etc [2, 3]. The most stable structure among them is c($5\sqrt{2} \times \sqrt{2}$)R45°, with $\Theta = 3/5$. In a condition such as b_{nat}, the ladder structure may exist partially on a surface even at $\Theta < 1/2$. This has been ascertained by our Monte Carlo simulation (MCS) [9], as follows.

We have conducted MCS and calculations of structure factors of the two-dimensional arrangements of adsorbed atoms obtained by MCS. We will present the details in [9]. We have found that the arced streaks could be reproduced in the condition $b_{\mathrm{nat}} < \sqrt{2}a$, while only a diffuse ring pattern could be obtained in the case of $b_{\mathrm{nat}} \geqslant \sqrt{2}a$. The former condition means that the atoms almost fill a triangular lattice on the surface with coverage $\Theta > 1/2$, if there is no

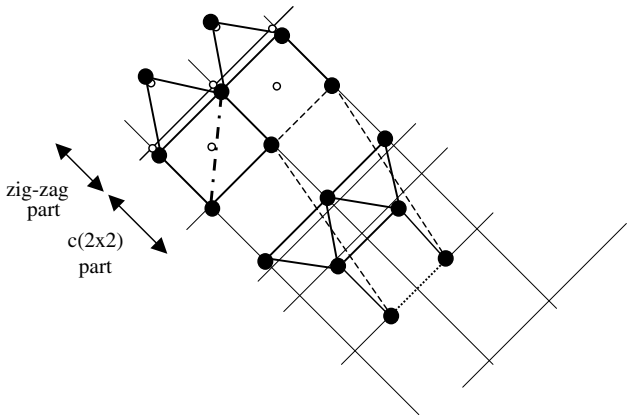

Figure 6. A shrunk and tilted second-neighbour pair of a c(2 × 2) unit (dashed and dotted line) inside a ladder structure. The zigzag part pushes and the c(2 × 2) part pulls one atom each of the pair. A unit cell of c($5\sqrt{2} \times \sqrt{2}$)R45° structure is also shown by dashed lines.

corrugation of the substrate potential. Hereafter, we choose the natural distance $b_{\mathrm{nat}} = 1.39a$, which corresponds to $\Theta = 3/5$ in the case where the atoms fill a surface.

(Notice that there are two types of coverages. There is a coverage when atoms fill a surface according to a value of b_{nat}. On the other hand, coverage by the usual definition is $\Theta \equiv N_{\mathrm{adatom}}/N_{\mathrm{substrate}}$, which is currently changed by experimental conditions. If we use the word 'coverage' without any modification, we intend the latter case.)

The atomic arrangement obtained by the MCS is as follows: the atoms have a complete 'ladder structure', ($5\sqrt{2} \times \sqrt{2}$)R45°, which fills a surface at $\Theta = 3/5$, as has been already observed experimentally [1] and by an energetic calculation at $T = 0$ K [3]. In the case of $\Theta < 3/5$, adsorbed atoms incompletely cover the surface. Exceptionally, at exactly $\Theta = 1/2$, a c(2 × 2) structure with complete occupancy is observed. At $\Theta < 1/2$, we observe a complex structure with incomplete occupancy including several c($5\sqrt{2} \times \sqrt{2}$)R45° clusters and several c(2 × 2) clusters. The last case, at $\Theta < 1/2$, results in the arced streak. Hereafter, we concentrate on the ladder structure unit.

The 'ladder' structure, c($5\sqrt{2} \times \sqrt{2}$)R45°, includes two parts (see figure 6). One is a zigzag part with bonds of '$d = a$'. The other is a c(2 × 2) part with bonds of '$d = \sqrt{2}a$'. Considering the actual bond lengths, the length '$d = a$' in the zigzag part is too short; hence, this bond is enlarged. On the other hand, the length '$d = \sqrt{2}a$' in the c(2 × 2) part is too long; hence, this pair, which is a diagonal line of the c(2 × 2) part, is shrunk and tilted.

These facts have been already observed in [1, 3]. Considering the diagonal line in a c(2×2) unit (see figure 6 again), which is a second-neighbour pair of the c(2×2) structure, it is inclined and shrunk, by the same factors mentioned above. That is, we can see the stability of the shrunk and tilted second-neighbour pair of the c(2 × 2) unit.

Moreover, we must explain the coherency of the diffraction by such pairs in obtaining strong and sharp diffraction streaks. Such pairs can exist any place on a surface. Thus, these pairs make parallel reflected planes for the Bragg reflection (see figure 7). These pairs have the structure factor

$$S(\vec{k}) = \mathrm{e}^{\mathrm{i}\vec{k}\cdot\vec{r}_{P1}} + \mathrm{e}^{\mathrm{i}\vec{k}\cdot\vec{r}_{Q1}} + \mathrm{e}^{\mathrm{i}\vec{k}\cdot\vec{r}_{P2}} + \mathrm{e}^{\mathrm{i}\vec{k}\cdot\vec{r}_{Q2}},$$

where atoms named $P_1, Q_1, \ldots$ in figure 7 are chosen. If we take $\vec{r}_{P1} = 0$, and define $\vec{r}_{Q1} - \vec{r}_{P1} = \vec{d}$, $\vec{r}_{P2} - \vec{r}_{P1} = \vec{r}_{Q2} - \vec{r}_{Q1} = \vec{\ell}$, then the structure factor is redefined to

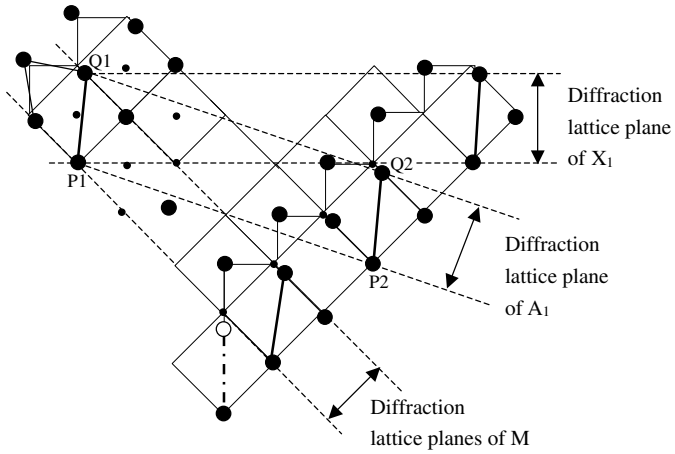

Figure 7. Plural ladder structures in a surface. Plural atomic pairs with shrinking and tilting, make reflected parallel planes for the Bragg reflection. An atom with an open circle and a pair with dotted and dashed lines are used later in section 5. These show the situation explained by figure 8.

$$S(\vec{k}) = \mathrm{e}^{\mathrm{i}\vec{k}\cdot\vec{0}} + \mathrm{e}^{\mathrm{i}\vec{k}\cdot\vec{d}} + \mathrm{e}^{\mathrm{i}\vec{k}\cdot\vec{\ell}} + \mathrm{e}^{\mathrm{i}\vec{k}\cdot(\vec{\ell}+\vec{d})}. \tag{3}$$

Further, if we take a condition such as $\vec{k}_\ell \cdot \vec{\ell} = 0$ (hereafter we denote $\vec{k}$ as $\vec{k}_\ell$ under various conditions), then $S(\vec{k}) = 2 + 2\mathrm{e}^{\mathrm{i}k_\ell d\cos\theta}$. Moreover, if we take a second condition such as $k_\ell d\cos\theta = 2\pi$, we obtain $S(\vec{k}) = 4$, which is the maximum value of the structure factor. These two conditions show that an end point of the vector $\vec{k}_\ell$ is on a line perpendicular to $\vec{d} \equiv P_i Q_i$, with the restriction that $k_\ell \cos\theta = 2\pi/d = \text{const}$.

If sufficient numbers of atoms with these pairs of $\vec{d}$ exist on the above reflected planes, then a strong and sharp diffraction streak can be seen.

Thus, the diffraction pattern with streaks seen in figure 5 is obtained again with a strong intensity and sharpness.

4. Origin of the arced shape

However, the streaks in figure 5 do not have arc shape yet; they are still straight lines. To obtain the arc shape, a variety of directions of the second-neighbour pairs is needed. Thus, we can first consider whether a bond with a diagonal direction, which is the y-direction, must exist in the case where a pair with '$d = a$' exists only on one side of a zigzag array. Then the bond is shrunk in the y-direction without tilting (see figure 8).

Thus, a number of pairs shrunk in the y-direction as in figure 9 make reflected planes. They bring diffraction lines as in figure 10. Such pairs may make a diffraction pattern including X_2 (see figure 10), in which $k_y = \alpha_2 \times (2\pi/2a)$, where $\alpha_2 \approx 6/5$, which is a little lower than X_1 in the k_y-direction.

Until now, we have considered diffraction by two types of pairs, as shown in figures 6 and 7, and figures 8 and 9. The arc shape could be explained to some degree.

We should also explore the possible diffraction effect by different pairs, such that one pair is tilted as in figure 6 and the other pair is directed along the y-direction as in figure 8. Since these pairs give non-parallel reflection lines, they do not contribute to the diffraction pattern. Therefore, we need only to consider parallel reflected planes consisting of the same pairs on both edges. (If the same pair locates inside the planes, the intensity becomes larger.)

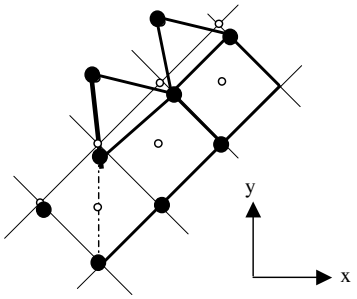

Figure 8. A shrunk atomic pair without tilting, inside a ladder structure. One bond with $d = a$ (a thick line) on the edge of the zigzag array pushes the pair, while no bond is found on the opposite side of the zigzag array.

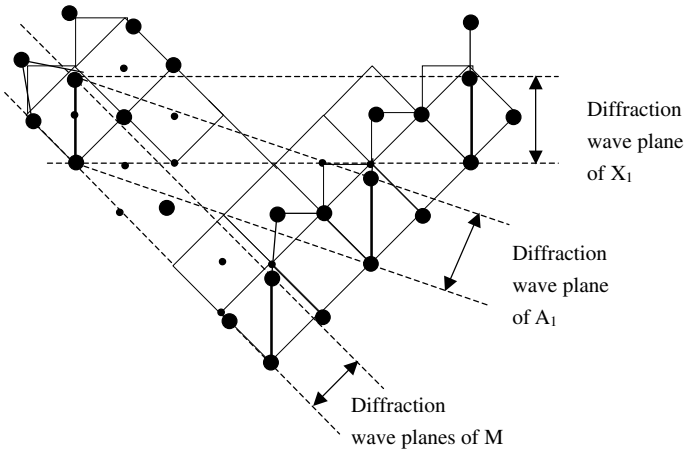

Figure 9. A number of atomic pairs with shrinking but not tilting make reflected parallel planes for the Bragg reflection.

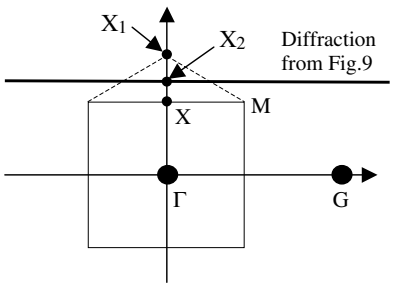

Figure 10. The diffraction pattern obtained from the atomic pairs in figure 9.

What we must consider next are parallel planes with a variety of pairs on both edges. Here, we assume the following arrangement of pairs: (i) a pair has unique length, R, $d = R = (1/\alpha_2) \times (2a)$, $\alpha_2 \approx 6/5$, besides (ii) a pair is tilted between a certain angles as $-\varphi_C \leqslant \varphi \leqslant \varphi_C$. Namely, each pair has only one parameter, a tilted angle, φ (see figure 11).

It is sufficient to consider an ensemble of pairs with a tilted angle, φ, where $-\varphi_C \leqslant \varphi \leqslant \varphi_C$. (The number of pairs with each angle φ, in this ensemble, we will discuss in the next

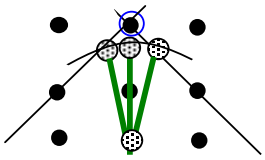

Figure 11. The assumed arrangement of atomic pairs, where the length is constant while the inclination is restricted to $-\varphi_C \leqslant \varphi \leqslant \varphi_C$.

(This figure is in colour only in the electronic version)

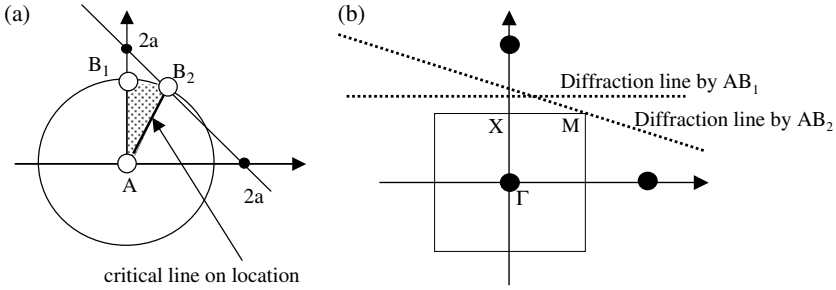

Figure 12. Correspondence between various types of pairs in (a) and diffraction lines in (b).

section.) Each pair with a certain angle φ gives a diffraction line, by the process shown in figure 7 or figure 9. Needless to say, a case of $\varphi = \varphi_C$ corresponds to figures 6 and 7, while a case of $\varphi = 0$ corresponds to figures 8 and 9.

In detail, the pair is shown by lines in figure 12(a). The tilted one with $\varphi = \varphi_C$ is a critical line which corresponds to figure 6 or 7. The vertical one with $\varphi = 0$ corresponds to figures 8 and 9. Such pairs bring diffraction lines in figure 12(b).

All of the diffraction lines may form an envelope function, which we study in the next section. This envelope function may be the pattern that is observed experimentally.

Rigorously speaking, we must modify this assumption that the pair takes unique length, namely $d = R$. It must be changed to $d = R(\varphi)$. However, the relation between figures 12(a) and (b) is definite. Then, there is only a quantitative change of locations of diffraction lines as in figure 12(b). Further, the envelope function, which is discussed later, is also changed only quantitatively. Thus, hereafter we take the above assumption.

5. Envelope function and diffraction lines

It is easy to obtain an envelope function, which corresponds to $0 \leqslant \varphi < \varphi_C$, as

$$k_y = \sqrt{\left(\frac{2\pi}{R}\right)^2 - k_x^2}, \qquad \text{at} \quad 0 \leqslant k_x < k_x^M. \tag{4}$$

On the other hand, a pair with $\varphi = \pm\varphi_C$ is not included in the envelope function, but only produces a straight line in diffraction space, as

$$k_y = Ak_x + B, \qquad \text{at } k_x^M \leqslant k_x \leqslant \pi/a. \tag{5}$$

We denoted the above notations as $A = -\frac{1-\sqrt{R^2/2-1}}{1+\sqrt{R^2/2-1}}$, $B = \frac{2\pi}{1+\sqrt{R^2/2-1}}$, and $k_x^M = \frac{2\pi}{R}\{1 - \sqrt{R^2/2-1}\}$. These lines are shown in figure 13.

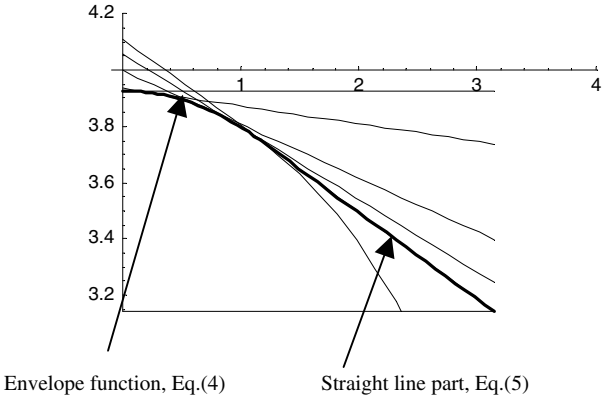

Figure 13. The envelope function originates from a bond tilted over $-\varphi_C \leqslant \varphi \leqslant \varphi_C$, and the line part from the limitation bond angle $\varphi = \varphi_C$. Notice that the scales of the horizontal line and the vertical line are different.

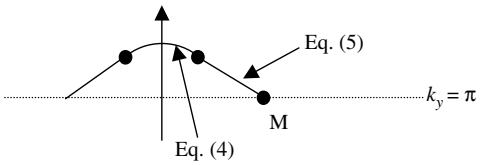

Figure 14. Schematic graph of (one-quarter of) the pattern, where horizontal and vertical scales are almost accurate.

The number of diffraction lines is infinite at the envelope part, $|\varphi| < \varphi_C$, while there is only one line at the $|\varphi| = \varphi_C$ part. Then the former envelope part seems to be stronger because the possible number of original diffraction lines is larger. However, the latter may contribute strongly from the experiment. We will explain this explanation by two steps.

In the first step, the number of tilted pairs ($|\varphi| = \varphi_C$) inside one cluster with zigzag array, as seen in figure 7, is larger than the number of pairs of y-direction, $|\varphi| = 0$ (see a dashed and dotted pair in figure 7), because the latter ones can locate only on both ends of a zigzag array. Thus, the line part according to $|\varphi| = \varphi_C$ gives stronger intensity compared with the other part.

In the next step, we consider the orientation angle may slightly change, as discussed in the previous section. We consider the two types of pairs separately; one is inside one cluster with the zigzag array, and the other at both the ends of the cluster. Most of the pairs inside the cluster basically have the angle, $|\varphi| = \varphi_C$; however, a few pairs vary the angle as $|\varphi| \leqslant \varphi_C$. On the other hand, pairs at the ends of the cluster may vary the angle as $0 \leqslant |\varphi| < \varphi_C$, where a possibility of $|\varphi| \approx 0$ may be large.

Therefore, the envelope function part (curved part) cannot give strong intensity relatively, in spite of the large number of diffraction lines. Even the above estimation on the ratio of both types of pairs is wrong; it only affects the intensities of the envelope part and the straight part. The shape as in figure 13 may not be changed.

The envelope part and line parts are shown schematically in figure 14. Then, the shape in figure 14 is almost the same as one-quarter of the diffraction pattern in figure 1.

Observing in detail the features of figure 1, it is possible to distinguish the envelope part and the line part to some degree. In addition, the line part looks more intense compared with the central curved part; the latter corresponds to the envelope function. This proves the stability

and a large number of the shrunk and tilted atomic pairs in the ladder structure as in figures 4, 6 and 7.

6. Conclusion

We observed the condition that the natural distance between adsorbed atoms, b_{nat}, is less than $\sqrt{2}a$; in particular, $b_{\mathrm{nat}} = 1.39a$ is consistent with the formation of arced streaks. In this condition, adsorbed atoms fill the surface and form a $(5\sqrt{2} \times \sqrt{2})\mathrm{R}45^\circ$ structure, which is a 'ladder structure', at $\Theta = 3/5$. Even at $\Theta < 1/2$, the atoms locally form a 'ladder structure'. In the ladder structure, the second-neighbour distance of the $\mathrm{c}(2 \times 2)$ unit (its normal distance is $d = 2a$) is shortened and tilted, especially by the existence of the zigzag part of the ladder structure.

Since the shortening and tilting of the atomic pairs occurs in many parts, greater intensity and sharpness of the arced streaks are expected.

In detail, tilted and shrunk pairs oriented in the same direction give only straight streaks, in which the direction of the streak is perpendicular to the pairs. Next, we can consider atomic pairs that are not tilted or that have a smaller angle than the above tilted one. Here, we can suppose the pairs have the same length, while their angles measured from the y-axis are in the region $-\varphi_{\mathrm{C}} \leqslant \varphi \leqslant \varphi_{\mathrm{C}}$. Therefore, each pair brings a straight steak in a diffraction space with a variety of inclinations. Thus, we can see that the envelope function of the straight streaks is nothing but the arced streak observed in the experiment.

References

[1] Jiang H, Mizuno S and Tochihara H 1997 *Surf. Sci.* **385** L930
[2] Mitani H, Hayashi T, Terasaki D, Chen M-S, Mizuno S and Tochihara H 2001 *Surf. Sci.* **493** 106
[3] Mitani H 1999 *Surf. Sci.* **438** 207
[4] Aruga T, Tochihara H and Murata Y 1985 *Surf. Sci.* **158** 490
[5] Shuster R, Barth J V, Ertl G and Behm R J 1991 *Surf. Sci.* **247** L229
Shuster R, Barth J V, Ertl G and Behm R J 1991 *Phys. Rev.* B **44** 13689
[6] Shirasawa T, Mizuno S and Tochihara H 2005 *Phys. Rev. Lett.* **94** 195502
[7] Higashi S, Ohshima T, Mizuno S and Tochihara H 2005 private communication
[8] Mitani H, Mizuno S, Tochihara H and Hayashi T 2005 *J. Phys. Soc. Japan* **74** 2663
[9] Hayashi T and Mitani H 2005 *e-J. Surf. Sci. Nanotechnol.* **3** 492